Published in final edited form as:
Colloids Surf B Biointerfaces. 2014 July 1; 119: 38–46. doi:10.1016/j.colsurfb.2014.04.022.

ATR-FTIR Spectroscopic Evidence for Biomolecular Phosphorus and Carboxyl Groups Facilitating Bacterial Adhesion to Iron Oxides

Sanjai J. Parikh[a,*], **Fungai N.D. Mukome**[a], and **Xiaoming Zhang**[a]

[a]Department of Land and, Air and Water Resources, University of California - Davis, One Shields Avenue, Davis, CA 95616

Abstract

Attenuated total reflectance (ATR) Fourier transform infrared (FTIR) spectroscopy has been used to probe the binding of bacteria to hematite (α-Fe_2O_3) and goethite (α-FeOOH). *In situ* ATR-FTIR experiments with bacteria (Pseudomonas putida, P. aeruginosa, Escherichia coli), mixed amino acids, polypeptide extracts, deoxyribonucleic acid (DNA), and a suite of model compounds were conducted. These compounds represent carboxyl, catecholate, amide, and phosphate groups present in siderophores, amino acids, polysaccharides, phospholipids, and DNA. Due in part to the ubiquitous presence of carboxyl groups in biomolecules, numerous IR peaks corresponding to outer-sphere or unbound (1400 cm^{-1}) and inner-sphere (1310-1320 cm^{-1}) coordinated carboxyl groups are noted following reaction of bacteria and biomolecules with α-Fe_2O_3 and α-FeOOH. However, the data also reveal that the presence of low-level amounts (i.e., 0.45-0.79%) of biomolecular phosphorous groups result in strong IR bands at ~1043 cm^{-1}, corresponding to inner-sphere Fe-O-P bonds, underscoring the importance of bacteria associated P-containing groups in biomolecule and cell adhesion. Spectral comparisons also reveal slightly greater P-O-Fe contributions for bacteria (*Pseudomonad, E. coli*) deposited on α-FeOOH, as compared to α-Fe_2O_3. This data demonstrates that slight differences in bacterial adhesion to Fe oxides can be attributed to bacterial species and Fe-oxide minerals. However, more importantly, the strong binding affinity of phosphate in all bacteria samples to both Fe-oxides results in the formation of inner-sphere Fe-O-P bonds, signifying the critical role of biomolecular P in the initiation of bacterial adhesion.

Keywords

ATR-FTIR spectroscopy; bacterial adhesion; biofilm; goethite; hematite

1. Introduction

Bacterial adhesion and the initiation of biofilm formation are critical processes for a wide variety of industrial and environmental processes. The effective development of soil

*corresponding author, sjparikh@ucdavis.edu; phone: 530-752-1265 .

Appendix A. Supplementary Data Supplementary data associated with this article can be found, in the online version.

bioremediation strategies, improved water treatment facilities, and reduced biofouling of pipelines require a comprehensive understanding of microbial interactions with solid surfaces. Bacterial adhesion to mineral surfaces can be initiated by biomolecules which are membrane bound or present in the extracellular polymeric substances (EPS). Although proteinaceous moieties (e.g., enzymes) are believed important for cell adhesion to negatively charged surfaces [1,2], binding to positively charged surfaces (e.g., metal oxides at environmental pH values) is likely facilitated by carboxyl groups [3-5], catecholate [6-8], and phosphate [1,5,9,10] groups associated with the EPS or cell surfaces. Included in the EPS are extracellular deoxyribonucleic acid (DNA), containing phosphodiester bonds, which have been shown to be key components in microbial biofilms [11].

Due to the high affinity of P for Fe-oxides, a number of P-containing functional groups originating from phospholipids, extracellular DNA, lipopolysaccharides, and other biomolecules all provide potential binding sites to initiate bacterial adhesion to metal-oxide surfaces. The favorable, and strong, interactions of phosphate with Fe-oxide surfaces have been well documented in numerous spectroscopic studies [5,12-15]. Regarding biomolecular P-groups, Omoike et al. used a combined attenuated total reflectance (ATR) Fourier transform infrared (FTIR) spectroscopy and modeling approach to demonstrate the occurrence of Fe-O-P bonds for extracted EPS reacted with goethite (α-FeOOH) and suggested that phosphodiester bonds in DNA mediate this process [9]. Another study revealed that phospholipid interactions with both α-FeOOH and hematite (α-Fe_2O_3) are facilitated by inner-sphere coordination of phosphate groups [13]. The importance of bimolecular-P interactions with Fe-oxides was also demonstrated with ATR-FTIR for live bacterial adhesion to α-Fe_2O_3 [5,10].

Although there is a growing evidence for biomolecular phosphate groups mediating cell adhesion to Fe-oxides, carboxyl groups present in EPS and on cell surfaces can also be important for cell adhesion to minerals. Recent studies by Gao and coworkers demonstrate that carboxyl groups mediate adhesion of *Cryptosoridium parvum* oocysts to a α-Fe_2O_3 [3,16]. The binding mechanisms of carboxyl groups in amino acids [17-20] and carboxylic acids [21-23] to metal-oxides has been well studied; with the inner-sphere complexes favored at slightly acidic pH [3,21,23,24].

Siderophores released by bacteria could also play an integral role in initiation of cell adhesion to Fe-oxides. For example, *E. coli* produces the siderophore enterobactin (salicylate and catecholate groups) [7] and *P. aeruginosa* produces pyoverdine (carboxyl, hydroxyl, hydroxamate, and catecholate groups) that readily bind Fe^{3+} [6,8] and have been shown to mediate cell adhesion to metal oxides surfaces [6-8], primarily through inner-sphere binding of catecholate groups to metals (e.g., Fe, Ti). Studies of model siderophores (i.e., desferroxamine B [DFOB], aerobactin) with lepidocrocite (γ-FeOOH) demonstrate possible inner-sphere sorption mechanisms through hydroxamate and outer-sphere coordination via carboxyl groups [25]. Another study on DFOB sorption to goethite, has revealed that following binding, DFOB can undergo metal-enhanced hydrolysis and promote the dissolution of the mineral surface [26].

The primary objective of the current study is to investigate the mechanisms of bacterial adhesion to Fe-oxides, with particular emphasis given to comparing the potential interactions of biomolecular carboxyl, catecholate, and phosphate groups. To conduct this research, ATR-FTIR spectroscopy has been used to investigate the binding of *P. aeruginosa*, *P. putida*, and *E. coli* and a suite of model compounds, mixed amino acids and peptides, and DNA to α-Fe_2O_3 and α-FeOOH films on an internal reflection element (IRE). The model compounds were chosen to consider the possible interactions of reactive functional groups present in siderophores, amino acids, polysaccharides, phospholipids, and DNA.

2. Experimental Methods

2.1 Chemical supplies

All solutions and suspensions were prepared in acid-washed lab-ware using 18.2 MΩ·cm Barnstead Nanopure water. Sample pH was adjusted with 100 mmol L^{-1} NaOH or HCl. Casamino acids (CA; Fisher Scientific; mixture of free amino acids), tryptone (Fisher Scientific; amino acids with oligopeptides present), and deoxyribonucleic acids (DNA; fish sperm) were used for experiments. In addition, commercially available model compounds were also used to aid in spectral interpretation of mixed systems. These compounds include L-glutamic acid (GA; Sigma-Aldrich), L-arginine (Sigma-Aldrich), L-dopamine (Sigma Aldrich), 4-guanidinobutyric acid (GBA; Sigma-Aldrich), benzoic acid (BA; Sigma-Aldrich), catechol (Sigma-Aldrich), ethylenediamine (EDA; Fisher Scientific), inosine-5′-monophosphate (IMP; Arcos Organics), and alginic acid (AA; Arcos Organics). Chemical structures for these compounds are given in the appendix (Appendix Fig. A1). In order to mimic the high functional group concentration present when bacteria encounter a surface, each compound was dissolved in 10 mmol L^{-1} NaCl at a concentration of 8 mg mL^{-1} and adjusted to pH 7 ± 0.2. Due to lower compound solubility the concentrations of DNA, AA, and BA were set at 5, 4.5, and 2.5 mg mL^{-1}, respectively. Additional experiments with GA were also conducted at 1.6 and 0.15 mg mL^{-1} to compare the impact of aqueous concentration on FTIR spectra following reaction with α-Fe_2O_3. Concentrations of C and N in model compounds (1 mg) were determined by total combustion (Costech ECS 4010). Total dissolved P in aqueous samples of model compounds was determined by persulfate digestion [27].

2.2 Bacteria and cultivation conditions

P. putida (GB-1), *P. aeruginosa* (PAO1, PDO300), and *Escherichia coli* (80LIS, 90SHS, 78SHS) were used in the current study. These generic *E. coli* strains were collected from the San Joaquin-Sacramento Delta (Table A2). Bacteria suspensions were prepared using previously established methods [10]. Briefly, bacteria strains were inoculated into Luria broth growth media and grown aerobically (at 150 rpm) at 25 °C to the early stationary phase (~10^5 cell mL^{-1}). After 24 h, cells were harvested by centrifugation (3000 RCF, 20 min, 4° C), washed with 10 mmol L^{-1} NaCl, and resuspended to 10^5 cell mL^{-1} in 10 mmol L^{-1} NaCl.

2.3 Fe-oxide synthesis and analysis

Synthesis of α-Fe_2O_3 followed Schwertmann and Cornell [28], which entailed dropwise addition of 100 mL of 1.0 mmol L^{-1} $Fe(NO_3)_3$ to 1 L of boiling water for 4 h and cooling overnight at room temperature. Excess nitrate was removed by flocculation (100 mmol L^{-1} NaCl) and supernatant discarded (four times). Particles were suspended in water (pH 4) and dialyzed (Fisherbrand regenerated cellulose; 3,500 MWCO) with exterior water (pH 4) changed twice daily. Dialysis was complete when the electrical conductivity and pH were unchanged over a 12 h period.

Synthesis of α-FeOOH was based on the method by Atkinson et al. [29]. Briefly, 20 mL increments of 2.5 mol L^{-1} KOH were added to 825 mL of 0.146 mol L^{-1} $Fe(NO_3)_3 \cdot 9H_2O$ until pH 12. The solution was then aged at 60 °C for 24 h. The precipitant was centrifuged and washed thrice with 1 mmol L^{-1} HCl (30,000 RCF, 20 min). Particles were suspended in water and dialyzed as discussed for α-Fe_2O_3.

X-ray diffraction (XRD) was performed using a Rigaku Ultima IV with a Cu X-ray source (40 kV, 40 mA). Transmission electron microscopy (TEM) was carried out on a Philips CM12 100 kV electron microscope after depositing particles onto 300 mesh copper grids coated with lacey formvar/carbon (Ted Pella, Inc.). A Bruker RFS 100/s Fourier-transform (FT) Raman spectrometer with a frequency doubled Nd:YAG laser (operating at 1064 nm) was used to collect Raman spectra (256 scans, 100 mW, 4 cm^{-1} resolution). Fourier transform infrared (FTIR) spectra of the Fe-oxide particles were collected by: 1) diffuse reflectance (DRIFT; PIKE Technologies EasiDiff) with 10% α-Fe_2O_3 (air dried) diluted with KBr (DTGS detector); 2) single bounce attenuated total reflectance (ATR) using a diamond internal reflection element (IRE) (PIKE Technologies GladiATR; DTGS detector); and 3) multi-bounce ATR-FTIR with a 45° ZnSe ATR crystal (HATR, PIKE Technologies) of dried suspension. All FTIR spectra in this study were collected using a Thermo Nicolet 6700 FTIR spectrometer (Thermo Scientific; 128 scans, 4 cm^{-1} resolution).

2.4 Bacteria and Biomolecule interactions: ATR-FTIR spectroscopy

Spectra of bacteria and biomolecule samples were collected after deposition on the ZnSe IRE and also onto a α-Fe_2O_3 or α-FeOOH coated IRE. Spectra for all bacteria on both Fe-oxide minerals were collected; however, based on these results and from biomolecule deposition on α-Fe_2O_3, only selected biomolecules (i.e., GA, DNA, CA, tryptone) were reacted with α-FeOOH. A bacteria suspension (1 mL, 10^5 cell mL^{-1}) or biomolecule solution (2.5 – 8.0 mg mL^{-1}) at pH 7 (± 0.1) in 10 mmol L^{-1} NaCl was deposited on the IRE. Spectra were collected every 15 min for a period of 2 h (spectra unchanged) and final pH determined (pH 7.0 ± 0.5). Fe-oxide coatings were prepared by depositing 1 mL of a 2 g L^{-1} mineral suspension on the ZnSe IRE and dried overnight and gently rinsed with water to remove loosely adhered material. Fe-oxide coatings were prepared for each experiment. Appropriate background spectra (i.e., 10 mmol L^{-1} NaCl, Fe-oxide coating) and all experiments were conducted a minimum of two times. Analysis of IR spectra for model compounds included calculation of Δψ of carboxylates by determining the separation distances between peaks corresponding to asymmetric carboxylate [$\psi_{as}(COO^-)$] and

symmetric carboxylate [$\psi_s(COO^-)$] stretching vibrations [i.e., $\Delta\psi = \psi_{as}(COO^-) - \psi_s(COO^-)$] [30-32].

3. Results and Discussion

3.1 Analysis of α-Fe_2O_3 and α-FeOOH Particles

The synthesis of α-Fe_2O_3 and α-FeOOH was confirmed via XRD, TEM, FT-Raman, and FTIR (Appendix Fig. A2 and A3). X-ray diffraction patterns show a variety of sharp peaks with d-spacings consistent with those previously observed for crystalline α-Fe_2O_3 [33] and α-FeOOH [28]. TEM micrographs reveal particles of 5 to 12 nm with a hexagonal morphology often considered diagnostic for α-Fe_2O_3 [28,33,34] and 1 to 4 μm needle shaped particles, characteristic of α-FeOOH [28]. FT-Raman spectra confirm crystalline α-Fe_2O_3 and α-FeOOH [35,36]. The α-Fe_2O_3 DRIFT, andATR, spectra display peaks at 578 (525) and 480 (443) cm^{-1} corresponding to Fe-O vibrations in α-Fe_2O_3 [28,34] and IR bands at 892 and 792 cm^{-1} are diagnostic for OH bending modes in α-FeOOH [28,37].

3.2 Bacterial Attachment to α-Fe_2O_3 and α-FeOOH

FTIR spectra of *P. aeruginosa* (PAO1, PDO300), *P. putida* (GB-1), and *E. coli* strains on a ZnSe IRE and α-Fe_2O_3 coated IRE have distinct bands corresponding to proteinaceous, carbohydrate, and phosphate moieties (Fig. 1, 2 and Appendix Table A3). Spectra of bacteria samples on ZnSe are similar (Fig. 1a and 2a). Minor differences include a peak at 1027 cm^{-1} for *E. coli* which is absent for *Pseudomonad* species and a band at 1147 cm^{-1} in all *E. coli* spectra is shifted to 1157 cm^{-1} for *Pseudomonad* species. Specific identification of these peaks is difficult as this region has a number of C-O, C-C, and P-O vibrations which overlap between 1000 to 1300 cm^{-1} [38]. Regardless, overall these spectra are similar and resemble those of various bacteria from the literature [10,39,40]. Since ATR-FTIR measures IR absorbing molecular bonds at the IRE interface (depth of penetration is ~1 μm), the spectra is biased towards the composition of cell exteriors [e.g., 2]. Therefore these results suggest that the EPS and exterior composition of these bacteria are chemically similar.

At environmentally relevant pH values bacteria typically exhibit a net negative charge [41] and the point of zero charge (PZC) of the ZnSe IRE is < 4 [42]. Therefore, adhesion of bacteria and biomolecules to ZnSe at pH 7 is limited and spectra represent unbound/aqueous phase samples. However, the PZC for α-Fe_2O_3 and α-FeOOH are typically around 8.5 and 7.5, respectively [43,44], and thus these Fe-oxides are primarily positively charged at pH 7. Therefore binding interactions between bacteria and these minerals are electrostatically favored.

The shifts in band locations (Fig. 1b-c, 2b-c) in spectra after depositing cells on α-Fe-oxide films is indicative of bacteria or biomolecule binding [45]. Although there are some notable differences in the spectra of bacteria on the α-Fe_2O_3 and α-FeOOH coatings, the general trends are consistent for all bacteria on both surfaces. Of most significance is the reduced intensity of the $\upsilon_{as}(PO_2^-)$ band (1230 cm^{-1}) with the appearance of an IR band at ~1040 cm^{-1} that has been observed in prior studies examining EPS and bacterial adhesion to Fe-oxides, and attributed to phosphate groups from biomolecules binding to Fe [5,9,10]. Similar

peaks were also previously observed for aqueous Fe(III)-phosphonate complexes of methylphosphonic acid (MPA), aminomethylphosphonic acid, and *N*-phosphonomethylglycine (glycophosphate) [46] and for MPA on α-FeOOH [12]. The most notable difference between bacteria on the two Fe-oxides is that the α-FeOOH spectra have less relative contributions from the amide and carboxyl peaks (1350-1800 cm^{-1}) and a new peak centered at 1041 cm^{-1} dominates the spectra. There is more separation between the peaks arising from C-C and C-O vibrations (~1081 cm^{-1}) and the Fe-O-P peak (~1040 cm^{-1}), suggesting a greater Fe-O-P binding for bacterial on α-FeOOH.

The IR band at 1400 cm^{-1}, which represents $\upsilon_s(COO^-)$, is present in spectra of bacteria on ZnSe and both Fe-oxides. In spectra of bacteria deposited on the Fe-oxide films, the fact that this prominent peak remains suggests a substantial amount of unbound, or outer-sphere coordinated, carboxyl groups are present. However, increased spectral intensity assigned to $\upsilon_s(COO^-)$ is noted between 1299-1309 cm^{-1} for the *Psedomonads* species and 1313-1319 cm^{-1} for *E. coli*, translating to a $\upsilon_s(COO^-)$ peak shift ranging from 81 to 101 cm^{-1}. The identification of inner-sphere complexes between COO^- and surfaces is determined by shifts (25 to 150 cm^{-1}) in the frequency of $\upsilon_s(COO^-)$ and $\upsilon_{as}(COO^-)$ relative to a spectrum of the aqueous adsorptive [e.g., 47,48,49]. Similar shifts have been observed for carboxylic acids reacted with TiO_2, ZrO_2, Al_2O_3, and Ta_2O_5 films [31]. This evidence suggests that inner-sphere complexation of bacterial carboxyl groups occurs during bacterial adhesion to the Fe-oxide films.

Carboxylate binding mechanisms can often be inferred through the separation differences ($\Delta\psi$) between the asymmetric carboxylate [$\psi_{as}(COO^-)$] and symmetric carboxylate [$\psi_s(COO^-)$] stretching vibrations [i.e., $\Delta\psi = \psi_{as}(COO^-) - \psi_s(COO^-)$] [30-32]. The typical ranges of $\Delta\nu$ for chelating bidentate, bridging bidentate, and monodentate binding are 60 to 100 cm^{-1}, 150 to 180 cm^{-1}, and >200 cm^{-1}, respectively [22,32]. However, separation distances can also be evaluated by comparing the $\Delta\nu$ of unbound carboxylate groups ($\Delta\nu_{ionic}$) with those representing metal-carboxyl complexes ($\Delta\nu_{com}$) such that $\Delta\nu_{com} > \Delta\nu_{ionic}$ for monodentate binding, $\Delta\nu_{com} < \Delta\nu_{ionic}$ for bridging bidentate, and $\Delta\nu_{com} << \Delta\nu_{ionic}$ for chelating bidentate [50]. Although the use $\Delta\nu$ to determine carboxyl coordination on mineral surfaces has previously been used to evaluate bacteria [4] and oocyst [3] binding to hematite, this approach was developed for simple organic acids and additional verification via chemical modelling approaches for chemically heterogeneous systems is warranted. Therefore, at present the use of $\Delta\nu$ for bacteria binding should only be used to suggest potential binding mechanisms which are an average for all carboxyls present in the system. In the current study, for the new peak at 1299-1319 cm^{-1}, $\Delta\nu$ ranges from 230 to 247 cm^{-1} for bacteria on α-Fe_2O_3 and α-FeOOH surfaces and thus suggests monodentate coordination. However, overlapping bands for the amide I and the $\psi_{as}(COO^-)$ centered at 1550 cm^{-1} in spectra of bacteria samples may further compromise this analysis of carboxylate coordination. [3,4]

The current data highlight the combined importance of carboxyl and phosphate moieties in live cell adhesion to Fe-oxide surfaces. As the binding of phosphate groups to Fe-oxide centers is typically favored over carboxyl groups [41,46] it is possible that phosphate moieties could serve to anchor cells, allowing for increased interaction with carboxyl groups

present on bacteria surfaces. This is in agreement with a prior ATR-FTIR study (*Shewanella putrefaciens* on α-Fe_2O_3) where P-containing functional groups initiated cell adhesion with cell wall proteins and carboxyl group peaks increasing with reaction time [5]. This is also supported by an atomic force microscopy study which showed that, at pH 7, the bond strength of phosphate groups to a hydrous Fe-oxide (~115 nN) exceeded the bond strength of carboxyl groups (~90 nN) to the same surface [51]. These results are also in general agreement with surface complexation models for metal adsorption to bacteria [52-54] and for bacteria to binding corundum [55]. In these studies, considerations of metal interactions with bacteria carboxyl groups was determined to be critical for the modeling the binding [xe.g., 53,55]; however, phosphate groups were also found to be important for metal binding at low bacteria:metal ratios and as the pH of the system increased toward pH 7 [52,56].

3.3 Analysis of Biomolecules and Model Compounds Interactions with Fe-oxides

Reactive functional groups present in amino acids, siderophores, and nucleic acids are investigated through the use of a suite of model compounds (Appendix Fig. A1), mixed amino acids and peptides, and DNA. Due to the defined composition of these biomolecules, and greater clarity of IR spectra, careful analysis of IR spectra can be used to evaluate potential binding mechanisms for bacteria. Of the biomolecules studied, tryptone and CA (both digests of casein) are the most heterogonous. Tryptone is a mixture of polypeptides with few free amino acids, whereas CA are mainly free amino acids with few peptides - both representing biomolecule mixtures with some P content [57,58]. Analysis of experimental solutions for the current study reveal P contributions to CA and tryptone are 0.45 and 0.79%, respectively (Table A1). AA is also an extracted biomolecule and has some impurities as observed from its 0.40% N content (Table A1). DNA also represents extracted biopolymers of nitrogenous nucleosides with a sugar backbone linked via phosphodiester bonds. Knowledge regarding the precise structures of model compounds permits exploration of the roles of specific functional groups, and group arrangements, in bacterial and biomolecular adhesion.

3.3.1. Biomolecule Binding—Similar to bacterial attachment to α-Fe_2O_3 and α-FeOOH, increased peak intensities were observed following biomolecule deposition on these Fe-oxide films (e.g., for α-Fe_2O_3 in Appendix Fig. A5). For the targeted biomolecules (i.e., tryptone, CA, DNA, GA) reacted with α-FeOOH films similar results were noted. Although not quantitative, increasing peak intensity can be used as a qualitative measure for sorption to the solid interface [45]. Due to the fact that CH_2 groups are not expected to bind to the Fe-oxide surfaces, bands assigned to CH_2 (i.e., 1454-1484 cm^{-1}) are used to estimate biomolecule concentration on the IRE surface. Utilizing IR bands around 1450 cm^{-1}, the increase in the peak absorbances on the α-Fe_2O_3-coated IRE (compared to ZnSe) demonstrate compound accumulations at the coated IRE-water interface.

3.3.2. Carboxyl Involvement in Binding—Analysis of FTIR spectra of bacteria deposited on α-Fe_2O_3 and α-FeOOH indicate that cell adhesion occurs, in part, through COO^- groups. Model compounds with COO^- groups have therefore been used to evaluate their potential role in cell adhesion to Fe-oxide surfaces. Spectra for these model compounds (BA, GA, arginine, GBA) and amino acid and polpeptide mixtures (CA, tryptone) reveal

increased peak intensities, compared to ZnSe, indicating sorption with the Fe-oxide coated IREs (Fig. 3ab, 4c, 5 and Appendix Fig. A4b-d). Investigations of GA interaction with α-Fe_2O_3 as a function of GA concentration (8, 1.6, 0.15 mg mL^{-1}) did not result in noticeable differences to the IR spectra (Appendix Fig. A6), and therefore concentration does not impact surface coordination to α-Fe_2O_3, as has been shown for GA on rutile [17,59].

Although the spectra of BA, GA, arginine, and GBA on ZnSe and following reaction with α-Fe_2O_3 (and α-FeOOH for GA) are similar, slight shifts in COO^- suggest inner-sphere complexation. Analysis of Δψ for the carboxyl region is complicated due to the prevalence of C-N and N-H bonds which absorb in the same region as $\psi_{as}(COO^-)$. Since BA has no overlapping bands, Δψ can be reliably calculated, decreasing from 154 ($\Delta\nu_{ionic}$) to 139 cm^{-1} ($\Delta\nu_{com}$) and indicate bidentate bridging coordination. GA, arginine, and GBA have too much spectral influence from C-N and N-H bonds for confident analysis of Δψ.

Inner-sphere binding is typically accompanied by a shift or splitting in the $\upsilon_s(COO^-)$ band (~1400 cm^{-1}) and is favored below pH ~6 [3,21,23,24] and, therefore, outer-sphere complexation is favored under the current experimental conditions (pH 7). And indeed, in spectra of bacteria on α-Fe_2O_3 and α-FeOOH, the unchanged IR band at 1400 cm^{-1} suggests outer-sphere, or unbound, carboxyl groups (Fig. 1b,c and 2b,c). However, the appearance of an IR band between 1299 and 1319 cm^{-1} following bacteria deposition on the Fe-oxide coatings are indicative of inner-sphere binding. These bands are not observed for BA, GA, arginine, and GBA on the Fe-oxide films and thus fail to represent the carboxyl groups reacting with bacteria and EPS on Fe-oxides.

The carboxyl region of tryptone and CA spectra have a number of similarities to the bacteria spectra. The $\upsilon_s(COO^-)$ band (~1400 cm^{-1}) remains following reaction with α-Fe_2O_3 (Fig 3a,b) and α-FeOOH (Fig. 5) and a small band appears at ~1305 cm^{-1}. Consistent with the bacteria spectra, this suggests a combination of both inner-sphere and outer-sphere carboxyl coordination to the Fe-oxides. The $\Delta\nu$ changes from 160 ($\Delta\nu_{ionic}$) to 245 cm^{-1} ($\Delta\nu_{com}$) for tryptone and from 119 ($\Delta\nu_{ionic}$) to 226 cm^{-1} ($\Delta\nu_{com}$) for CA. Following prior interpretations, this corresponds to monodentate carboxyl coordination [3,4,22,32], which was also observed for bacteria deposited on the Fe-oxide films. However, like bacteria, these samples contain carboxyl groups in diverse chemical environments and the FTIR spectra represent the average absorbances of the carboxyl groups.3.3.3. Catecholate Binding to α-Fe_2O_3. FTIR spectra of catechol and dopamine on α-Fe_2O_3 are notably different from the corresponding solution phase spectra (ZnSe) and suggest a change in molecular conformation concomitant with binding to the α-Fe_2O_3 (Fig. 4b and Appendix Fig. A4a). The resulting spectra have sharp bands at ~1480 and 1260 cm^{-1} present only for corresponding α-Fe_2O_3 spectra. This indicates inner-sphere coordination of catecholate groups with α-Fe_2O_3, and is consistent with prior studies examining catechol and siderophore (pyoverdine, enterobactin) sorption to TiO_2 and Fe_2O_3 [6-8]. The fact that these peaks are not present in spectra of bacteria reacted with Fe-oxides (Fig. 3, 4) suggest that catecholate groups are not fundamental for bacteria attachment in this case. Siderophore production by bacteria is typically induced under conditions of Fe scarcity [60] and in studies where siderophores are involved in cell adhesion Fe was purposefully omitted to enhance siderophore production [6,8]. In the

current study, bacteria were cultivated with excess Fe, possibly explaining the absence of significant contributions from siderophores to spectra of bacteria on the α-Fe_2O_3 surface.

3.3.4. Amine Interactions with α-Fe_2O_3—Although the PZC of α-Fe_2O_3 is around 8.0, and α-Fe_2O_3 is primarily positively charged at pH 7 [43], some deprotonated sites will be present interactions with amine groups. The relative increase in peak intensities for model compounds with NH_2 groups (i.e., GBA, GA, dopamine, arginine) following reaction with α-Fe_2O_3 is indicative of sorption; however, contributions from NH_2 groups are believed to be minimal and complexation via carboxyl groups (i.e., GBA, GA, arginine) and catecholate groups (dopamine) dominate the interactions for the model compounds studied.

Further evidence of the limited interaction between NH_2 and α-Fe_2O_3 is observed via examination of EDA (Fig. 4d). The spectrum for EDA arises from the IR absorption of C-C, C-H, C-N, and N-H bonds, all of which are present in bacteria. Since EDA has no carboxyl or phosphate groups, IR bands attributed to NH_2 and CH_2 are easily examined. The relative increase of the aliphatic band at ~1460 cm^{-1} on the α-Fe_2O_3 film is the lowest for all biomolecules studied (Appendix Fig. A5) and indicates that EDA does not have a high affinity for the Fe-oxide surface. It is asserted that contributions from amine groups in bacteria do not play a significant role in cell adhesion to Fe-oxides under the conditions studied. The results from the current study are in general agreement with Barja and Afonso [46], who demonstrated that the interaction of glyphosphate (*N*-phosphomethylglycine) with α-FeOOH is facilitated via inner-sphere Fe-phosphonate complexes with no coordination of carboxylate and amino groups with the surface (pH 3 to 9).

3.3.5. Phosphate Mediated Binding—Phosphate in IR spectra of bacteria and biomolecules on ZnSe is noted by peaks between 1247 and 1213 cm^{-1}. For biomolecules, this is most noticeable for DNA (8.33% P) and IMP (6.03% P) (Appendix Table A1; Fig 3c, 4a) with small peaks noted for CA and tryptone (both < 1% P) (Fig. 3a,b). Following reaction with the Fe-oxide films, the spectra of tryptone and CA at wavenumbers below 1100 cm^{-1} are altered (Fig. 3a,b,c, 4a, 5) and most closely match spectral patterns for bacteria cells on α-Fe_2O_3 and α-FeOOH (Fig. 1b, 2b). These spectra have a broad IR band, attributed to Fe-O-P [5,9,10,12], between 1037-1066 cm^{-1} with spectral contributions at 1078/1087 and 989 cm^{-1}. These peaks are similar to bands at approximately ~1070, 1040, and 990 cm^{-1} present in all corresponding bacteria spectra. In the tryptone and CA spectra, only minor IR bands are observed between 1200 and 1000 cm^{-1} for data acquired with ZnSe; however, there is a large increase in relative peak intensity in this region following interaction with α-Fe_2O_3 and α-FeOOH. The fact that CA and tryptone have < 1% P content and IR bands corresponding to Fe-O-P are produced stresses the importance of this interaction.

4. Conclusions

The data presented in this study demonstrate the importance of P-containing and carboxyl groups in bacterial adhesion to an ATR crystal coatings of α-Fe_2O_3 and α-FeOOH. The high affinity of phosphate for Fe-oxides at pH 7 results in prominent IR bands corresponding to Fe-O-P molecular vibrations for model compounds with P contents as low as 0.45%. These

FTIR spectroscopic analyses with bacteria and biomolecules make evident the critical role of phosphate containing functional groups in bacterial adhesion to both α-Fe_2O_3 and α-FeOOH surfaces. Evidence is also provided for additional mechanisms which assist cell binding to the Fe-oxide surfaces via combined outer- and inner-sphere (monodentate) sorption of carboxyl groups. Although increased P-O-Fe contributions on α-FeOOH (compared to α-Fe_2O_3) during bacterial adhesion are observed, the data suggest that overall mechanisms for cell attachment to these Fe-oxides are similar. The FTIR investigations of model compounds and amino acid and peptide mixtures also demonstrate the high affinity of P-containing functional groups for Fe-oxide surfaces in the presence of competing carboxyl, amine, and other prevalent bimolecular functional groups. In order to further enhance our understanding of bacterial adhesion process, additional experiments with additional amino acids and extracted P-containing biomolecules from bacteria and EPS should be conducted on a variety of metal-oxide and layer-silicate mineral surfaces.

Supplementary Material

Refer to Web version on PubMed Central for supplementary material.

Acknowledgments

The authors thank Dr. Sabyasachi Sen for FT-Raman spectrometer access, Dr. Randal Southard for XRD analysis, Timothy Doane for P measurements, Andrew Margenot for C and N measurements, and Dr. E.R. Atwill for providing the *E. coil* strains. Funding for Xiaoming Zhang was provided through the Kearney Foundation of Soil Science.

References

[1]. Cao YY, Wei X, Cai P, Huang QY, Rong XM, Liang W. Preferential adsorption of extracellular polymeric substances from bacteria on clay minerals and iron oxide. Colloids Surf. B. Biointerfaces. 2011; 83:122–127. [PubMed: 21130614]

[2]. Parikh SJ, Chorover J. FTIR spectroscopic study of biogenic Mn-oxide formation by *Pseudomonas putida* GB-1. Geomicrobiol. J. 2005; 22:207–218.

[3]. Gao X, Metge DW, Ray C, Harvey RW, Chorover J. Surface Complexation of Carboxylate Adheres Cryptosporidium parvum Oocysts to the Hematite-Water Interface. Environ. Sci. Technol. 2009; 43:7423–7429. [PubMed: 19848156]

[4]. Ojeda JJ, Romero-Gonzalez ME, Pouran HM, Banwart SA. In situ monitoring of the biofilm formation of *Pseudomonas putida* on hematite using flow-cell ATR-FTIR spectroscopy to investigate the formation of inner-sphere bonds between the bacteria and the mineral. Mineral. Mag. 2008; 72:101–106.

[5]. Elzinga EJ, Huang J-H, Chorover J, Kretzschmar R. ATR-FTIR Spectroscopy Study of the Influence of pH and Contact Time on the Adhesion of *Shewanella putrefaciens* Bacterial Cells to the Surface of Hematite. Environ. Sci. Technol. 2012; 46:12848–12855. [PubMed: 23136883]

[6]. McWhirter MJ, Bremer PJ, Lamont IL, McQuillan AJ. Siderophore-mediated covalent bonding to metal (oxide) surfaces during biofilm initiation by *Pseudomonas aeruginosa* bacteria. Langmuir. 2003; 19:3575–3577.

[7]. Upritchard HG, Yang J, Bremer PJ, Lamont IL, McQuillan AJ. Adsorption of Enterobactin to Metal Oxides and the Role of Siderophores in Bacterial Adhesion to Metals. Langmuir. 2011; 27:10587–10596. [PubMed: 21744856]

[8]. Upritchard HG, Yang J, Bremer PJ, Lamont IL, McQuillan AJ. Adsorption to metal oxides of the Pseudomonas aeruginosa siderophore pyoverdine and implications for bacterial biofilm formation on metals. Langmuir. 2007; 23:7189–7195. [PubMed: 17530790]

[9]. Omoike A, Chorover J, Kwon KD, Kubicki JD. Adhesion of bacterial exopolymers to a-FeOOH: inner-sphere complexation of phosphodiester groups. Langmuir. 2004; 20:11108–11114. [PubMed: 15568864]

[10]. Parikh SJ, Chorover J. ATR-FTIR spectroscopy reveals bond formation during bacterial adhesion to iron oxide. Langmuir. 2006; 22:8492–8500. [PubMed: 16981768]

[11]. Jakubovics NS, Shields RC, Rajarajan N, Burgess JG. Life after death: the critical role of extracellular DNA in microbial biofilms. Lett. Appl. Microbiol. 2013; 57:467–475. [PubMed: 23848166]

[12]. Barja BC, Tejedor-Tejedor MI, Anderson MA. Complexation of Methylphosphonic Acid With the Surface of Goethite Particles in Aqueous Solution. Langmuir. 1999; 15:2316–2321.

[13]. Cagnasso M, Boero V, Franchini MA, Chorover J. ATR-FTIR studies of phospholipid vesicle interactions with alpha-FeOOH and alpha-Fe2O3 surfaces. Colloids Surf. Biointerfaces. 2010; 76:456–467.

[14]. Olsson R, Giesler R, Loring JS, Persson P. Adsorption, Desorption, and Surface-Promoted Hydrolysis of Glucose-1-Phosphate in Aqueous Goethite (α-FeOOH) Suspensions. Langmuir. 2010; 26:18760–18770. [PubMed: 21087005]

[15]. Fang L, Cao Y, Huang Q, Walker SL, Cai P. Reactions between bacterial exopolymers and goethite: A combined macroscopic and spectroscopic investigation. Water Res. 2012; 46:5613–5620. [PubMed: 22921391]

[16]. Gao X, Chorover J. Amphiphile Disruption of Pathogen Attachment at the Hematite (α-Fe2O3)–Water Interface. Langmuir. 2011; 27:5936–5943. [PubMed: 21488611]

[17]. Parikh SJ, Kubicki JD, Jonsson CM, Jonsson CL, Hazen RM, Sverjensky DA, Sparks DL. Evaluating glutamate and aspartate binding mechanisms to rutile (α-TiO2) via ATR-FTIR spectroscopy and quantum chemical calculations. Langmuir. 2011; 27:1778–1787. [PubMed: 21235255]

[18]. Roddick-Lanzilotta AD, Connor PA, McQuillan AJ. An in situ infrared spectroscopic study of the adsorption of lysine to TiO2 from an aqueous solution. Langmuir. 1998; 14:6479–6484.

[19]. Roddick-Lanzilotta AD, McQuillan AJ. An in situ infrared spectroscopic study of glutamic acid and of aspartic acid adsorbed on TiO2: Implications for the biocompatibility of titanium. J. Colloid Interface Sci. 2000; 227:48–54. [PubMed: 10860593]

[20]. Norén K, Loring JS, Persson P. Adsorption of alpha amino acids at the water/goethite interface. J. Colloid Interface Sci. 2008; 319:416–428. [PubMed: 18155715]

[21]. Boily J-F, Nilsson N, Persson P, Sjöberg S. Benzenecarboxylate Surface Complexation at the Goethite (α-FeOOH)/Water Interface: I. A Mechanistic Description of Pyromellitate Surface Complexes from the Combined Evidence of Infrared Spectroscopy, Potentiometry, Adsorption Data, and Surface Complexation Modeling. Langmuir. 2000; 16:5719–5729.

[22]. Norén K, Persson P. Adsorption of monocarboxylates at the water/goethite interface: The importance of hydrogen bonding. Geochim. Cosmochim. Acta. 2007; 71:5717–5730.

[23]. Ha J, Hyun Yoon T, Wang Y, Musgrave CB, Brown JGE. Adsorption of Organic Matter at Mineral/Water Interfaces: 7. ATR-FTIR and Quantum Chemical Study of Lactate Interactions with Hematite Nanoparticles. Langmuir. 2008; 24:6683–6692. [PubMed: 18522441]

[24]. Hwang YS, Lenhart JJ. Adsorption of C4-Dicarboxylic Acids at the Hematite/Water Interface. Langmuir. 2008; 24:13934–13943. [PubMed: 19360935]

[25]. Borer P, Hug SJ, Sulzberger B, Kraemer SM, Kretzschmar R. ATR-FTIR spectroscopic study of the adsorption of desferrioxamine B and aerobactin to the surface of lepidocrocite (gamma-FeOOH). Geochim. Cosmochim. Acta. 2009; 73:4661–4672.

[26]. Simanova AA, Persson P, Loring JS. Evidence for ligand hydrolysis and Fe(III) reduction in the dissolution of goethite by desferrioxamine-B. Geochim. Cosmochim. Acta. 2010; 74:6706–6720.

[27]. Valderrama JC. The simultaneous analysis of total nitrogen and total phosphorus in natural waters. Marine Chemistry. 1981; 10:109–122.

[28]. Schwertmann, U.; Cornell, RM. Iron oxides in the Laboratory: Preparation and Characterization. 2nd ed. Wiley-VCH; Weinheim: 1991.

[29]. Atkinson RJ, Posner AM, Quirk JP. Adsorption of potential-determining ions at ferric oxide-aqueous electrolyte interface. J. Phys. Chem. 1967; 71:550–558.

[30]. Alcock NW, Tracy VM, Waddington TC. Acetates and acetato-complexes. 2. spectroscopic studies. Journal of the Chemical Society-Dalton Transactions. 1976:2243–2246.

[31]. Dobson KD, McQuillan AJ. In situ infrared spectroscopic analysis of the adsorption of aliphatic carboxylic acids to TiO2, ZrO2, Al2O3, and Ta2O5 from aqueous solutions. Spectrochim. Acta, Pt. A: Mol. Biomol. Spectrosc. 1999; 55:1395–1405.

[32]. Chu HA, Hillier W, Debus RJ. Evidence that the C-terminus of the D1 polypeptide of photosystem II is ligated to the manganese ion that undergoes oxidation during the S-1 to S-2 transition: An isotope-edited FTIR study. Biochemistry. 2004; 43:3152–3166. [PubMed: 15023066]

[33]. He YT, Wan JM, Tokunaga T. Kinetic stability of hematite nanoparticles: the effect of particle sizes. J. Nanopart. Res. 2008; 10:321–332.

[34]. Schwertmann, U.; Taylor, RM. Iron oxides. In: Klute, A., editor. Methods of Soil Analysis, Part 1 – Physical and Mineralogical Methods. Vol. Vol 5. SSSA; Madison, WI: 1989. p. 379-438.

[35]. Smith GD, Clark RJH. Raman microscopy in archaeological science. J. Archaeol. Sci. 2004; 31:1137–1160.

[36]. de Faria DLA, Venâncio Silva S, de Oliveira MT. Raman microspectroscopy of some iron oxides and oxyhydroxides. J. Raman Spectrosc. 1997; 28:873–878.

[37]. Cambier P. Infrared study of goethites of varying crystallinity and particle size; I, Interpretation of OH and lattice vibration frequencies. Clay Minerals. 1986; 21:191–200.

[38]. Nivens DE, Chambers JQ, Anderson TR, Tunlid A, Smit J, White DC. Monitoring Microbial Adhesion and Biofilm Formation by Attenuated Total Reflection Fourier-Transform Infrared Spectroscopy. J. Microbiol. Methods. 1993; 17:199–213.

[39]. Jiang W, Saxena A, Song B, Ward BB, Beveridge TJ, Myneni SCB. Elucidation of Functional Groups on Gram-positive and Gram-negative Bacterial Surfaces Using Infrared Spectroscopy. Langmuir. 2004; 20:11433–11442. [PubMed: 15595767]

[40]. McWhirter MJ, McQuillan AJ, Bremer PJ. Influence of ionic strength and pH on the first 60 min of *Pseudomonas aeruginosa* attachment to ZnSe and to TiO2 monitored by ATR-IR spectroscopy. Colloids Surf. B. Biointerfaces. 2002; 26:365–372.

[41]. Appenzeller BMR, Duval YB, Thomas F, Block JC. Influence of Phosphate on Bacterial Adhesion Onto Iron Oxyhydroxide in Drinking Water. Environ. Sci. Technol. 2002; 36:646–652. [PubMed: 11883420]

[42]. Tickanen LD, Tejedor-Tejedor MI, Anderson MA. Quantitative Characterization of Aqueous Suspensions Using Variable-Angle ATR-FTIR Spectroscopy: Determination of Optical Constants and Absorption Coefficient Spectra. Langmuir. 1997; 13:4829–4836.

[43]. Sposito, G. The Chemsitry of Soils. Second ed. Oxford University Press; New York: 2008.

[44]. Sverjensky DA. Zero-point-of-charge prediction from crystal chemistry and solvation theory. Geochim. Cosmochim. Acta. 1994; 58:3123–3129.

[45]. Sigg L, Goss KU, Haderlein S, Harms H, Hug SJ, Ludwig C. Sorption phenomena at environmental solid surfaces. Chimia. 1997; 51:893–899.

[46]. Barja BC, Afonso MD. Aminomethylphosphonic Acid and Glyphosate Adsorption Onto Goethite: a Comparative Study. Environ. Sci. Technol. 2005; 39:585–592. [PubMed: 15707059]

[47]. Gu BH, Schmitt J, Chen Z, Liang LY, Mccarthy JF. Adsorption and Desorption of Different Organic-Matter Fractions on Iron-Oxide, Geochim. Cosmochim. Acta. 1995; 59:219–229.

[48]. Duckworth OW, Martin ST. Surface Complexation and Dissolution of Hematite by C-1-C-6 Dicarboxylic Acids at pH=5.0. Geochim. Cosmochim. Acta. 2001; 65:4289–4301.

[49]. Kang S, Xing B. Adsorption of Dicarboxylic Acids by Clay Minerals as Examined by in Situ ATR-FTIR and ex Situ DRIFT. Langmuir. 2007; 23:7024–7031. [PubMed: 17508766]

[50]. Hug SJ, Bahnemann D. Infrared spectra of oxalate, malonate and succinate adsorbed on the aqueous surface of rutile, anatase and lepidocrocite measured with in situ ATR-FTIR. J. Electron. Spectrosc. Relat. Phenom. 2006; 150:208–219.

[51]. Kreller DI, Gibson G, Novak W, Van Loon GW, Horton JH. Competitive adsorption of phosphate and carboxylate with natural organic matter on hydrous iron oxides as investigated by chemical force microscopy. Colloids Surf. Physicochem. Eng. Aspects. 2003; 212:249–264.

[52]. Fein JB, Daughney CJ, Yee N, Davis TA. A Chemical Equilibrium Model for Metal Adsorption Onto Bacterial Surfaces. Geochim. Cosmochim. Acta. 1997; 61:3319–3328.

[53]. Yee N, Fein J. Cd adsorption onto bacterial surfaces: A universal adsorption edge? Geochim. Cosmochim. Acta. 2001; 65:2037–2042.

[54]. Yee N, Fein JB. Quantifying metal adsorption onto bacteria mixtures: A test and application of the surface complexation model. Geomicrobiol. J. 2003; 20:43–60.

[55]. Yee N, Fein JB, Daughney CJ. Experimental Study of the Ph, Ionic Strength, and Reversibilitybehavior of Bacteria-Mineral Adsorption. Geochim. Cosmochim. Acta. 2000; 64:609–617.

[56]. Daughney CJ, Fein JB, Yee N. A comparison of the thermodynamics of metal adsorption onto two common bacteria. Chem. Geol. 1998; 144:161–176.

[57]. Nolan RA, Nolan WG. Elemental analysis of vitamin-free casamino acids. Applied Microbiology. 1972; 24:290–291. [PubMed: 16349930]

[58]. Nolan RA. Amino acids and growth factors in vitamin-free casamino acids. Mycologia. 1971; 63:1231–1234. [PubMed: 5156995]

[59]. Sverjensky DA, Jonsson CM, Jonsson CL, Cleaves HJ, Hazen RM. Glutamate surface speciation on amorphous titanium dioxide and hydrous ferric oxide. Environ. Sci. Technol. 2008; 42:6034–6039. [PubMed: 18767662]

[60]. Crowley DE, Wang YC, Reid CPP, Szaniszlo PJ. Mechanisms of iron acquisition from siderophores by microorganisms and plants. Plant Soil. 1991; 130:179–198.

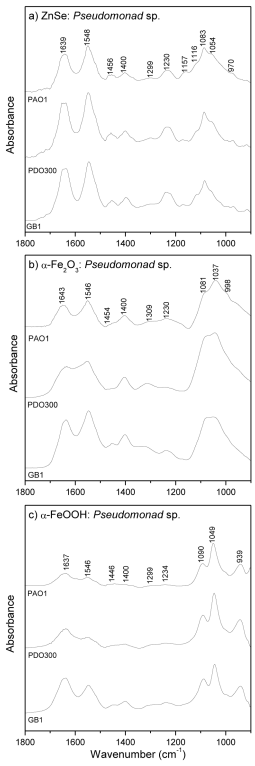

Fig. 1.

ATR-FTIR spectra of *P. aeruginosa* and *P. putda* collected on a) ZnSe and b) α-Fe_2O_3 coated ZnSe in 10 mmol L^{-1} NaCl at pH 7.

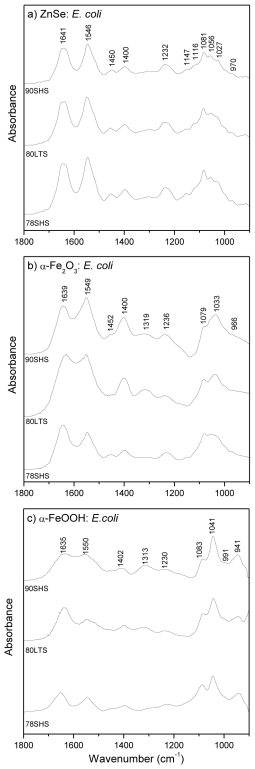

Fig. 2.

ATR-FTIR spectra of *E. coli* collected on a) ZnSe and b) α-Fe_2O_3 coated ZnSe in 10 mmol L^{-1} NaCl at pH 7.

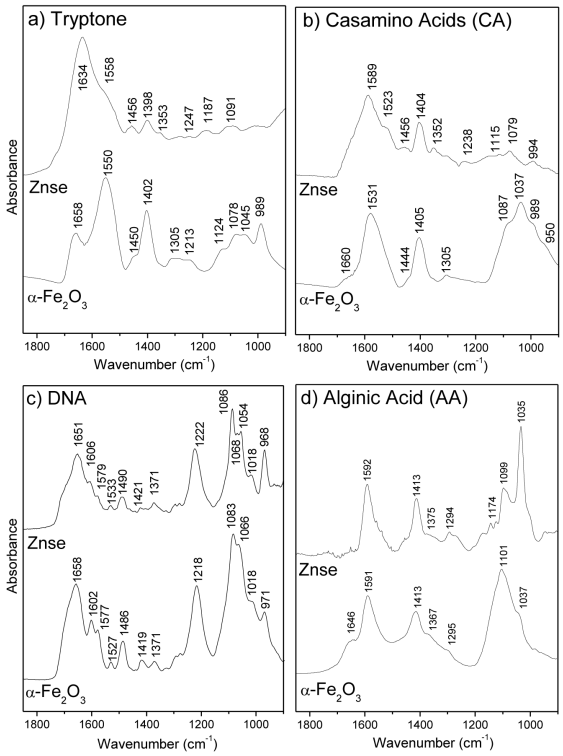

Fig. 3.

ATR-FTIR spectra of extracted biomolecules: a) tryptone, b) casamino acids, c) DNA, and d) alginic acid in 10 mmol L^{-1} NaCl at pH 7 on ZnSe and α-Fe_2O_3 coated ZnSe.

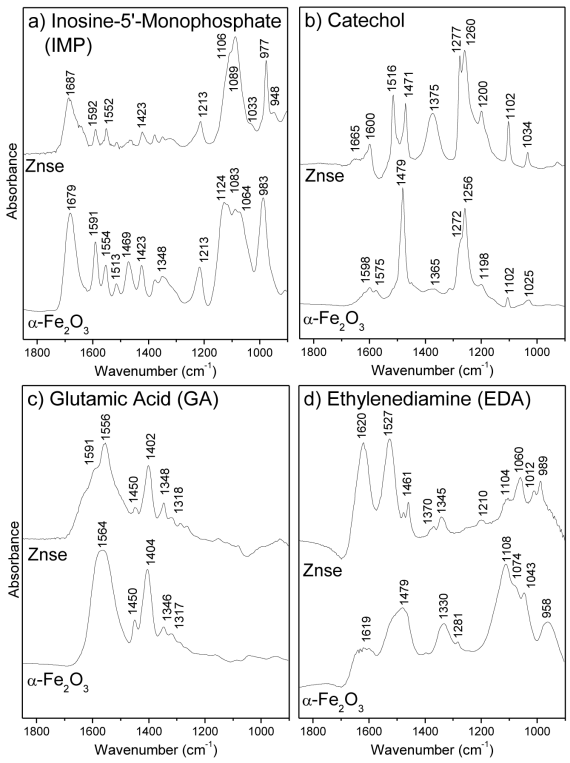

Fig. 4.

ATR-FTIR spectra of model biomolecules: a) inosine-5′-monophosphate, b) catechol, c) glutamic acid, and d) ethylenediamine acid in 10 mmol L^{-1} NaCl at pH 7 on ZnSe and α-Fe_2O_3 coated ZnSe.

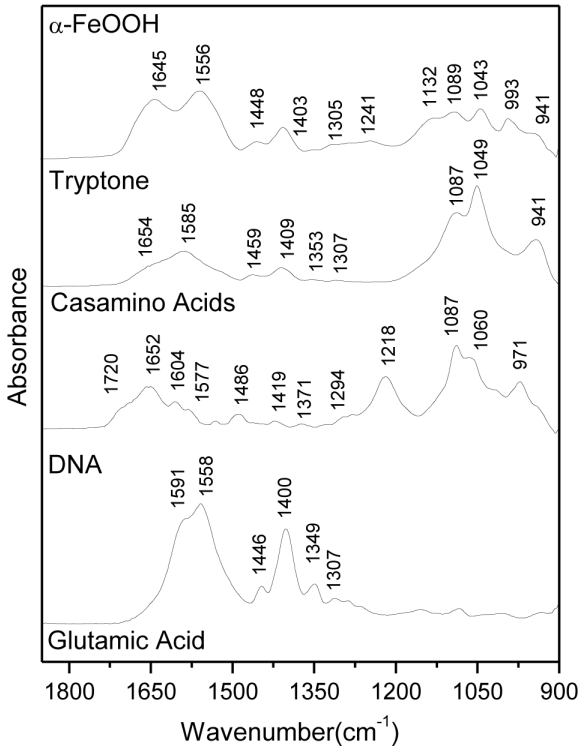

Fig. 5.

ATR-FTIR spectra of tryptone, casamino acids, DNA, and glutamic acid in 10 mmol L^{-1} NaCl at pH 7 on ZnSe and α-FeOOH coated ZnSe.